N65-12728 (ACCESSION NUMBER)

34 (PAGES)

CR59695 (NASA CR OR TMX OR AD NUMBER)

1 (THRU)

(CODE)

30 (CATEGORY)

FACILITY FORM 602

National Aeronautics and Space Administration
Washington 25, D. C.

Covering the period 20 July thru 19 October 1964

GEOPHYSICS CORPORATION OF AMERICA
Bedford, Massachusetts

PLANETARY METEOROLOGY

Quarterly Progress Report No. 2

Contract No. NASw-975

GPO PRICE $ ______

OTS PRICE(S) $ ______

Hard copy (HC) 2.00

Microfiche (MF) .50

CASE FILE COPY

TABLE OF CONTENTS

SECTION 1

INTRODUCTION

The general objective of the contract is to improve our knowledge of the meteorology of the planets Mars, Venus, and Jupiter. Primary emphasis is placed on the thermal state and circulation regimes in these planetary atmospheres.

Research during the past three months has been devoted to: 1) development and programming of a model for computing the vertical distribution of radiative equilibrium temperature from the surface to the top of a planetary atmosphere with a complete cloud cover (such as the Venus atmosphere); 2) study, development, and application of models for estimating average wind velocities and the general circulation characteristics of the atmosphere of Venus; 3) development of a model for computing the vertical distribution of radiative equilibrium temperature above the clouds of Jupiter; and, 4) estimation of maximum winds likely to be encountered near the surface of Mars.

SECTION 2

METEOROLOGY OF VENUS

2.1 RADIATIVE EQUILIBRIUM TEMPERATURE DISTRIBUTION IN THE VENUS ATMOSPHERE

In Quarterly Progress Report No. 1, a model was developed for computing the radiative equilibrium temperature distribution of the entire atmosphere of a planet, such as Venus, that has a complete cloud cover. It was assumed that the atmosphere above and below the cloud was grey in the infrared and that the cloud behaved as a black body for infrared radiation. The following radiative equilibrium conditions were applied: 1) the atmosphere above and below the cloud is in infrared radiative equilibrium, 2) the upward infrared radiative flux at the top of the atmosphere is equal to the incoming solar radiation, and 3) the net infrared radiative flux at the surface is equal to the incoming solar radiation. Application of these conditions led to equations for computing the vertical distribution of radiative equilibrium temperature. The necessary parameters and their adopted values were:

$T_e = 237^{\circ}K$	$\tau_g = 7.0$	$\tau_b = 6.86$
$T_o = 700^{\circ}K$	$\tau_c = 6.995$	

where T_e is the effective temperature of the incoming solar radiation, T_o is the surface temperature, τ_g is the infrared opacity of the entire atmosphere, τ_c is the infrared opacity level of the cloud-top, and τ_b is the infrared opacity level of the cloud-base. In the model, opacity increased upwards from a value of zero at the surface. The temperature distribution computed with this model was unrealistic. The temperatures in the sub-cloud layer were essentially isothermal at a value of about 696°K, while the temperatures in the above-cloud layer decreased from 237.3°K at the cloud-top to slightly less than 199°K at the top of the atmosphere; there was a temperature drop of 456°K from the cloud-base to the cloud-top. The unreasonable temperature distribution obtained with this model is probably largely due to the assumption of a completely black cloud cover. To remedy this defect, we are developing a model in which the cloud is not a perfect absorber of infrared radiation.

Let us retain the same basic model as before, but let us now assume that the cloud cover has an emissivity ϵ and a transmissivity $(1-\epsilon)$ for infrared radiation rather than an emissivity of 1 and a transmissivity of zero. The net flux of infrared radiation at any level τ above the cloud-top can now be written as

$$F(\tau) = 2\epsilon B_c E_3(\tau - \tau_c) + 2\int_{\tau_c}^{\tau} B(t)\, E_2(\tau - t)\,dt$$

$$+ \left[2B_o E_3(\tau_b) + 2\int_0^{\tau_b} B(t)\, E_2(\tau_b - t)\,dt\right](1-\epsilon)2E_3(\tau-\tau_c)$$

$$- 2\int_{\tau}^{\tau_g} B(t)\, E_2(t - \tau)\,dt \qquad (1)$$

where F is the net flux of infrared radiation, τ is infrared opacity, B is black body flux, the E's are exponential integrals, and the subscripts o, b, c, and g refer to the surface, the cloud-base, the cloud-top, and the top of the atmosphere, respectively.

The net flux of infrared radiation at any level below the cloud-top can now be written as

$$F(\tau) = 2B_o\, E_3(\tau) - 2\epsilon\, B_b\, E_3(\tau_b - \tau) + 2\int_o^{\tau} B(t)\, E_2(\tau - t)dt$$
$$- 2\int_{\tau}^{\tau_b} B(t)E_2(t-\tau)dt - \left[2\int_{\tau_c}^{\tau_g} B(t)E_2(\tau_g - t)dt\right](1-\epsilon)2E_3(\tau_b-\tau). \quad (2)$$

Applying the radiative equilibrium condition

$$\frac{dF}{d\tau} = 0, \quad (3)$$

we obtain the following relationships

Above cloud:

$$2B(\tau) = B_cE_2(\tau-\tau_c) + \int_{\tau_c}^{\tau_g} B(t)E_1(|\tau-t|)dt + 2\left[B_oE_3(\tau_b) + \int_o^{\tau_b} B(t)E_2(\tau_b-t)dt\right]$$
$$\cdot (1 - \epsilon)\ E_2(\tau - \tau_c) \quad (4)$$

Below cloud:

$$2B(\tau) = B_o\ E_2(\tau) + B_b\epsilon\ E_2(\tau_b-\tau) + \int_o^{\tau_b} B(t)\ E_1(|\tau-t|)dt$$
$$+ 2\left[\int_{\tau_c}^{\tau_g} B(t)\ E_2(\tau_g - t)dt\right](1 - \epsilon)\ E_2(\tau_b - \tau) \tag{5}$$

Applying the condition that the upward infrared radiative flux at the top of the atmosphere must balance the incoming solar radiation, we obtain

$$2\epsilon\ B_c E_3(\tau_g - \tau_c) + 2\int_{\tau_c}^{\tau_g} B(t)\ E_2(\tau_g - t)dt + \left[2B_o\ E_3(\tau_b)\right.$$
$$\left. + 2\int_o^{\tau_b} B(t)\ E_2(\tau_b-t)dt\right](1 - \epsilon)2E_3(\tau_g-\tau_c) = \sigma\ T_e^4 \tag{6}$$

where T_e is the effective temperature of the incoming solar radiation.

From the condition that the net fluxes of infrared radiation at the cloud-base and cloud-top are equal, we obtain

$$2B_oE_3(\tau_b) - \epsilon B_b + 2\int_o^{\tau_b} B(t)E_2(\tau_b-t)dt - 2\int_{\tau_c}^{\tau_g} B(t)E_2(\tau_g-t)dt\ (1-\epsilon) =$$
$$2\epsilon B_c + \left[2B_oE_3(\tau_b) + 2\int_o^{\tau_b} B(t)E_2(\tau_b-t)dt\right](1-\epsilon) - 2\int_{\tau_c}^{\tau_g} B(t)E_2(t-\tau_c)dt \tag{7}$$

Equations (4), (5), (6), and (7) provide a system of equations that can be solved numerically for the distribution of B and — since B is proportional to T^4 — the distribution of T above and below the clouds, and for the values of B and T at the cloud-base and cloud-top. The necessary input parameters are T_e, T_o, τ_g, τ_c, and τ_b. This model is currently being programmed for a computer and results are expected during the next quarter.

2.2 CIRCULATION STUDIES

In Quarterly Progress Report No. 1, we reported on the development of and computations with 1) a model for estimating the average horizontal velocity in the Venus atmosphere (Haurwitz model), and 2) a model for determining the circulation pattern in the Venus atmosphere (sea-breeze model). Both models considered Venus to be non-rotating. The resulting winds were due, in the first model, to a difference in radiational heating between sub-solar and anti-solar points, and, in the second model, to a temperature gradient between sub-solar and anti-solar points. For an appropriate range of the necessary parameters, the maximum wind velocities varied from 8 to 33 m/sec. During the past quarter, we have considered two other theoretical models for estimating the circulation characteristics of the Venus atmosphere. This work is summarized here.

First, a model due to Mintz (1962) is used to compute the mean wind velocity. Since Venus is considered as a synchronously rotating planet, the energy radiated to space in the dark hemisphere must be replaced by an energy transport across the terminator from the sunlit side. Using a simple two-layer model atmosphere and considering equal mass distribution in these two layers, Mintz obtained a formula for the mean wind velocities at the middle levels in each layer. In this model, the wind speeds at the middle level of the top layer are equal to the wind speeds at the middle level of the bottom layer, but the directions are opposite. His formula is

$$\left(\frac{4\pi a^2}{2}\right)\left[\sigma T_e^4\right] = \frac{\pi a R T_2 p_s}{gm}\left(1 - \frac{\gamma}{\gamma_d}\right) v_1$$

where a = radius of Venus.

p_s = surface pressure.

γ = vertical temperature gradient.

$\gamma_d = -\frac{g}{c_p}$ = adiabatic temperature gradient.

$T_2 = \frac{T_1 + T_3}{2}$ = temperature at middle level of the atmosphere

$(\ )_{1,2,3}$ = subscripts refer to the different levels of the atmosphere. Level 1 refers to the level at which pressure is 1/4 of surface pressure, p_s. Level 2 refers to the level at which $p = 1/2\ p_s$, etc.

σ = Stefan-Boltzmann constant.

R/m = gas constant for atmosphere with molecular weight, m.

g = gravitational acceleration.

T_e = infrared brightness temperature.

v_1 = velocity at pressure surface $1/4\ p_s$ at terminator.

The left hand side of the formula represents the outgoing energy in the dark hemisphere and the right hand side represents the energy that must be transported from the sunlit side. With the following data

p_s = 10 atm. $\qquad$ $R/m = 3\times10^6\ cm^2/sec^2\ deg$

$T_2 = 580^oK$ $\qquad$ $a = 6\times10^6\ m$

$T_e = 237^oK$ (Sinton, 1963) $\qquad$ $g = 8.4\ m/sec^2$

$\gamma/\gamma_d = 9/10$ $\qquad$ $\sigma = 5.7\times10^{-5} erg/cm^2/sec/deg^4$,

one obtains the velocity at level $\frac{3p_s}{4}$ to be

$$v_3 = -1.0\ m/sec\ ,$$

where the negative sign represents a wind direction toward the sub-solar point. If we extrapolate to the surface, the wind velocity would be twice this value, or

$$v_4 = -2.0\ m/sec.$$

This velocity is the smallest wind velocity we have obtained from any of the theoretical models used thusfar. In order to obtain a realistic estimate of the mean surface wind velocity, we must test and compare the results of all available models of the general circulation.

The following model of the circulation is based on a driving force due to a net gain of radiational energy at the sub-solar point and a loss of radiational energy at the anti-solar point. A two dimensional linear model is used — that is, the circulation is represented on a vertical plane extending from the sub-solar point to anti-solar point and the planet's curvature is neglected. Since the effect of rotation of Venus is negligible, motion is mainly in the meridional direction (here we define the meridional direction in the direction of lines joining the sub-solar and anti-solar points). To keep the mathematics tractable, the motion is assumed to start from relative rest. Then, the equations of motion, energy equation, and equation of continuity can be simply written as

$$\nu\nabla^2 v = -\frac{\partial\phi}{\partial y} \tag{8}$$

$$\frac{\partial\phi}{\partial p} = -\frac{RT}{p} \tag{9}$$

$$\kappa\nabla^2 T + \Gamma\omega = \frac{Q}{c_p} \tag{10}$$

$$\frac{\partial v}{\partial y} + \frac{\partial\omega}{\partial p} = 0 \tag{11}$$

where Q = non-adiabatic net heating.

c_p = specific heat at constant pressure.

ν,κ = eddy viscosity and eddy heat conductivity respectively, (here we assume $\nu/\kappa = 1$).

v = velocity in the meridional direction (in y-direction).

$\omega = \frac{dp}{dt}$ = vertical velocity in pressure coordinates system.

T,p = temperature and pressure respectively.

∇^2 = Laplacian operator.

Φ = geopotential height.

R = gas constant for Venusian atmosphere.

Γ = stratification factor $= \frac{T}{\theta}\frac{\partial\theta}{\partial p} = \frac{\partial T}{\partial p} + \left(\frac{\Gamma_d}{\partial p/\partial z}\right)$ (as a first approximation, Γ is assumed to be $- B_o/p_o$).

Γ_d = dry adiabatic lapse rate.

θ = potential temperature.

From the equation of continuity (11), we may write

$$v = \frac{\partial\psi}{\partial p}$$

and

$$\omega = - \frac{\partial\psi}{\partial y} \tag{12}$$

where ψ = stream function. Substituting Equation (12) into (8) and (10) and eliminating Φ by using Equation (9), we obtain

$$\nu\nabla^2 \frac{\partial^2\psi}{\partial p^2} = \frac{\partial T}{\partial y} \tag{13}$$

and

$$-\Gamma \frac{\partial^2\psi}{\partial y^2} + \nu\nabla^2 \frac{\partial T}{\partial y} = \frac{\partial Q}{\partial y}\frac{1}{c_p} . \tag{14}$$

If we approximate the eddy viscosity and heat conductivity by Rayleigh friction and Newtonian conductivity, i.e., by replacing $\nu\nabla^2$ by c, and eliminating T from Equation (13) and (14), we obtain

$$-\Gamma \frac{\partial^2\psi}{\partial y^2} + \frac{c^2 p}{R}\frac{\partial^2\psi}{\partial p^2} = \frac{\partial Q/\partial y}{c_p} . \tag{15}$$

Let $q = 2\left(\frac{p}{p_o}\right)^{\frac{1}{2}}$ and $\Gamma = -\frac{B_o}{p_o}$.

Equation (15) can be then written as

$$\frac{\partial^2 \psi}{\partial y^2} + \frac{c^2}{RB_o}\left(\frac{\partial^2 \psi}{\partial q^2} - \frac{1}{q}\frac{\partial \psi}{\partial q}\right) = \frac{P_o}{c_p B_o}\frac{\partial Q}{\partial y}. \qquad (16)$$

Let the net non-adiabatic heating, Q, as a function of latitude and pressure, be represented by

$$Q = DqJ_1(\alpha q)\left[N(y) - \frac{W}{D}\right]$$

where $D = S(1 - A) \Big/ \int_0^{p_o} qJ_1(dq)\frac{dp}{g}.$

S = the solar constant at Venus' distance from the sun.

A = the planetary albedo.

$q = 2\left(\frac{p}{p_o}\right)^{\frac{1}{2}}.$

$\alpha = 1.916$

p, p_o = pressure and surface pressure respectively.

$DN(y)$ = variation of absorption of solar radiation as a function of latitude alone.

W = long-wave radiation is a constant over all horizontal surfaces.

J_1 = Bessel function of the first kind of order one.

Further let

$\psi = DqJ_1(\alpha q)f$.

f = the horizontal distribution of stream function.

In the above definitions, the vertical profile of the net energy is assumed proportional to $qJ_1(\alpha q)$ and the horizontal distribution is assumed proportional to $N-\frac{W}{D}$ where N is assumed as a cosine function between $y=0$ and $y=\frac{1}{2}$ and zero between $y=\frac{1}{2}$ to $y=L$ as shown in Figure 1.

Substituting ψ and Q into Equation (16) and letting $\frac{\pi}{L}y = \varphi$ (φ representing the angle between sub-solar point and any point on the surface along the meridional direction), one obtains

$$\frac{\partial^2 f}{\partial \varphi^2} - \mu f = \lambda \frac{\partial F}{\partial \varphi} \tag{17}$$

where $\mu = \frac{\alpha^2 c^2 a^2}{RB_o}$, $\lambda = \frac{p_o a}{B_o c_p}$.

The function N can be approximated by a Fourier cosine series in a range between 0 and π as

$$N = \frac{a_o}{2} + \sum_{\ell=1}^{\infty} a_\ell \cos \ell\varphi \tag{18}$$

where $\frac{a_o}{2} = \frac{1}{\pi}$, $a_1 = \frac{1}{2}$

$$a_{\ell=2m} = \sum_{m=1}^{\infty} \frac{2(-1)^{m+1}}{(4m^2-1)\pi} \cos 2m\varphi, \qquad \text{at} \quad \ell \geq 2 .$$

The function f in ψ can be assumed as a Fourier sine series

$$f = \frac{2}{\pi} \sum_{n=1}^{\infty} b_n \sin n\varphi \tag{19}$$

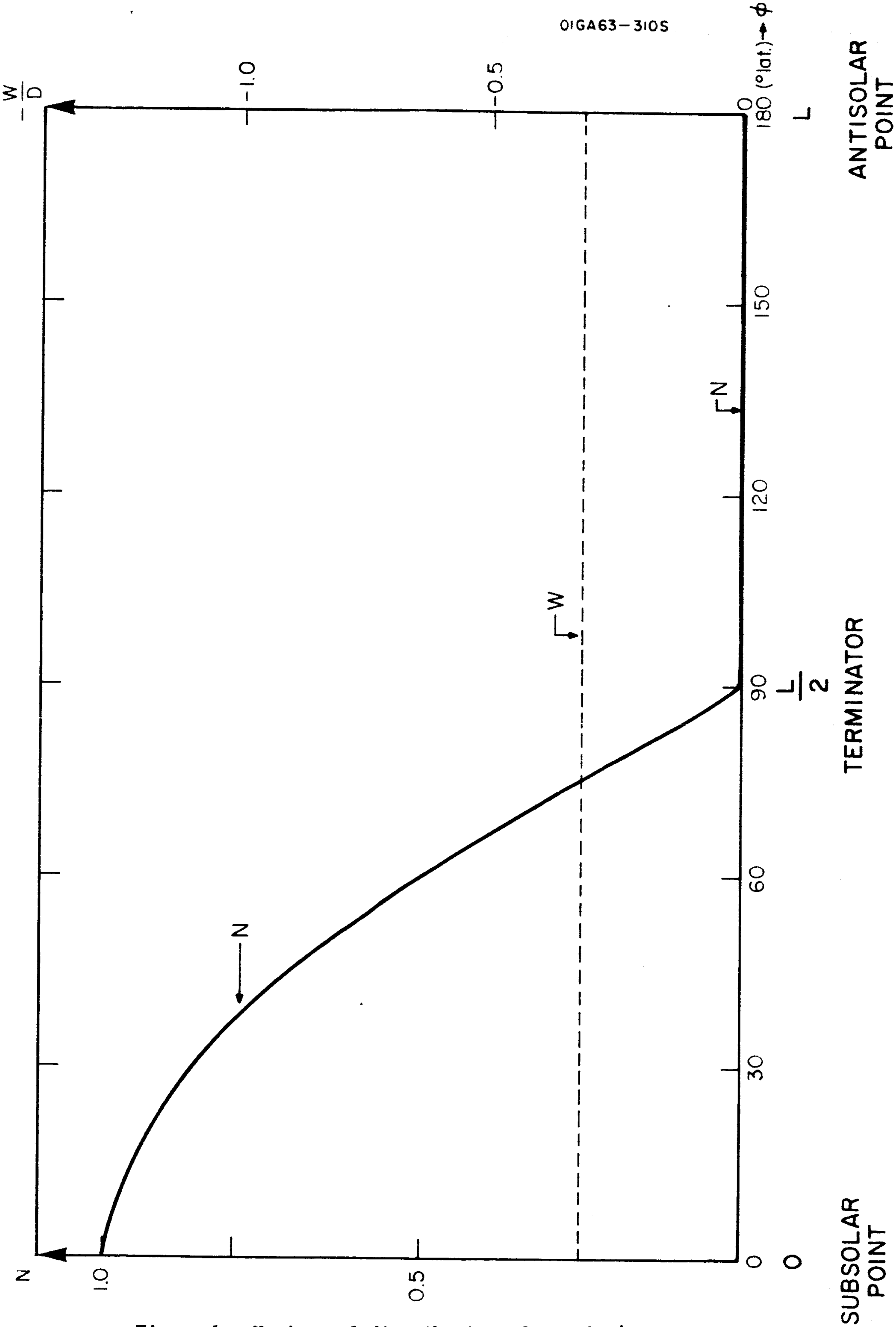

Figure 1. Horizontal distribution of N and W/D.

Substituting (18) and (19) into Equation (17), then multiplying sin $n\varphi$ and integrating φ from 0 to π, one obtains

$$-(n^2 + \mu)b_n = -\lambda n \left\{ \frac{\pi}{4}\delta + \sum_{m=1}^{\infty} \frac{(-1)^{m+1}}{(4m^2-1)} \right\}$$

or

$$b_n = \frac{\lambda n}{n^2+\mu} \left\{ \frac{\pi}{4}\delta + \sum_{m=1}^{\infty} \frac{(-1)^{m+1}}{(4m^2-1)} \right\} ; \qquad (20)$$

$$\delta = \begin{cases} 0 & , \quad n \neq 1 \\ 1 & , \quad n = 1 \end{cases} .$$

More explicitly

$$b_1 = \frac{\lambda}{1+\mu}\frac{\pi}{4}$$

$$b_2 = \frac{2\lambda}{3(4+\mu)}$$

$$b_4 = -\frac{4\lambda}{15(16+\mu)}$$

$$b_6 = \frac{6\lambda}{35(36+\mu)}$$

.

.

.

Therefore, the stream function ψ and velocity v can be written as

$$\psi = 2D\left(\frac{p}{p_o}\right)^{\frac{1}{2}} J_1\left[2\alpha\left(\frac{p}{p_o}\right)^{\frac{1}{2}}\right]\frac{2}{\pi}\left\{\frac{\pi}{4}\frac{\lambda}{1+\mu}\sin\varphi + \frac{2\lambda}{3(4+\mu)}\sin 2\varphi - \frac{4\lambda}{15(16+\mu)}\sin 4\varphi\right.$$
$$\left. + \frac{6\lambda}{35(36+\mu)}\sin 6\varphi - \frac{8\lambda}{63(64+\mu)}\sin 8\varphi + \;.\;.\;.\;.\;.\right\} \tag{21}$$

and

$$v = \frac{\partial\psi}{\partial p} = \frac{2\alpha D}{p_o} J_o\left[2\alpha\left(\frac{p}{p_o}\right)^{\frac{1}{2}}\right]\frac{2}{\pi}\left\{\frac{\pi}{4}\frac{\lambda}{1+\mu}\sin\varphi + \frac{2\lambda}{3(4+\mu)}\sin 2\varphi\right.$$
$$\left. - \frac{4\lambda}{15(16+\mu)}\sin 4\varphi + \;.\;.\;.\;.\;.\;.\;.\;.\;.\;.\right\} . \tag{22}$$

At the terminator, i.e. $\varphi = \frac{\pi}{2}$, Equation (22) becomes

$$v = \frac{D\alpha}{p_o} J_o\left[2\alpha\left(\frac{p}{p_o}\right)^{\frac{1}{2}}\right]\frac{\lambda}{1+\mu} . \tag{23}$$

With the same values of the parameters used in Quarterly Progress Report No. 1, D is about 3.5×10^{-6}cal/gm/sec. The computed wind velocities for this model and other models are shown in Table 1.

The first two results are obtained from Quarterly Progress Report No. 1. The present model yields a smaller wind velocity, which is close to that based on Mintz's model.

The horizontal distribution of v with latitude of the model (up to second harmonics) is shown in Figure 2. The stream function is plotted in Figure 3. It is seen that the maximum surface velocity is not at the

TABLE 1

Estimated surface level wind velocities in the Venus atmosphere obtained from different models.

Models	Velocity (m/sec)	Remarks
Sea Breeze Model	33	$\nu = \kappa = 10^7\ cm^2/sec$ (maximum velocity is at 7 km above surface).
Haurwitz's Model	18	$c = 10^{-5}/sec$; at surface and tropopause level.
Mintz's Model	2.0	$\frac{\partial T}{\partial z} = -8^o/km$; at surface and tropopause level.
Present Model		$c = 10^{-5}/sec$, $\frac{\partial T}{\partial z} = -8^o/km$, maximum value at $\varphi \approx 70^o$ lat.
	1.10	at surface level;
	2.75	at top of the atmosphere.
		$c = 10^{-5}/sec$, $\frac{\partial T}{\partial z} = -5^o/km$, maximum value at $\varphi \approx 70^o$ lat.
	0.20	at surface level;
	0.50	at top of the atmosphere.

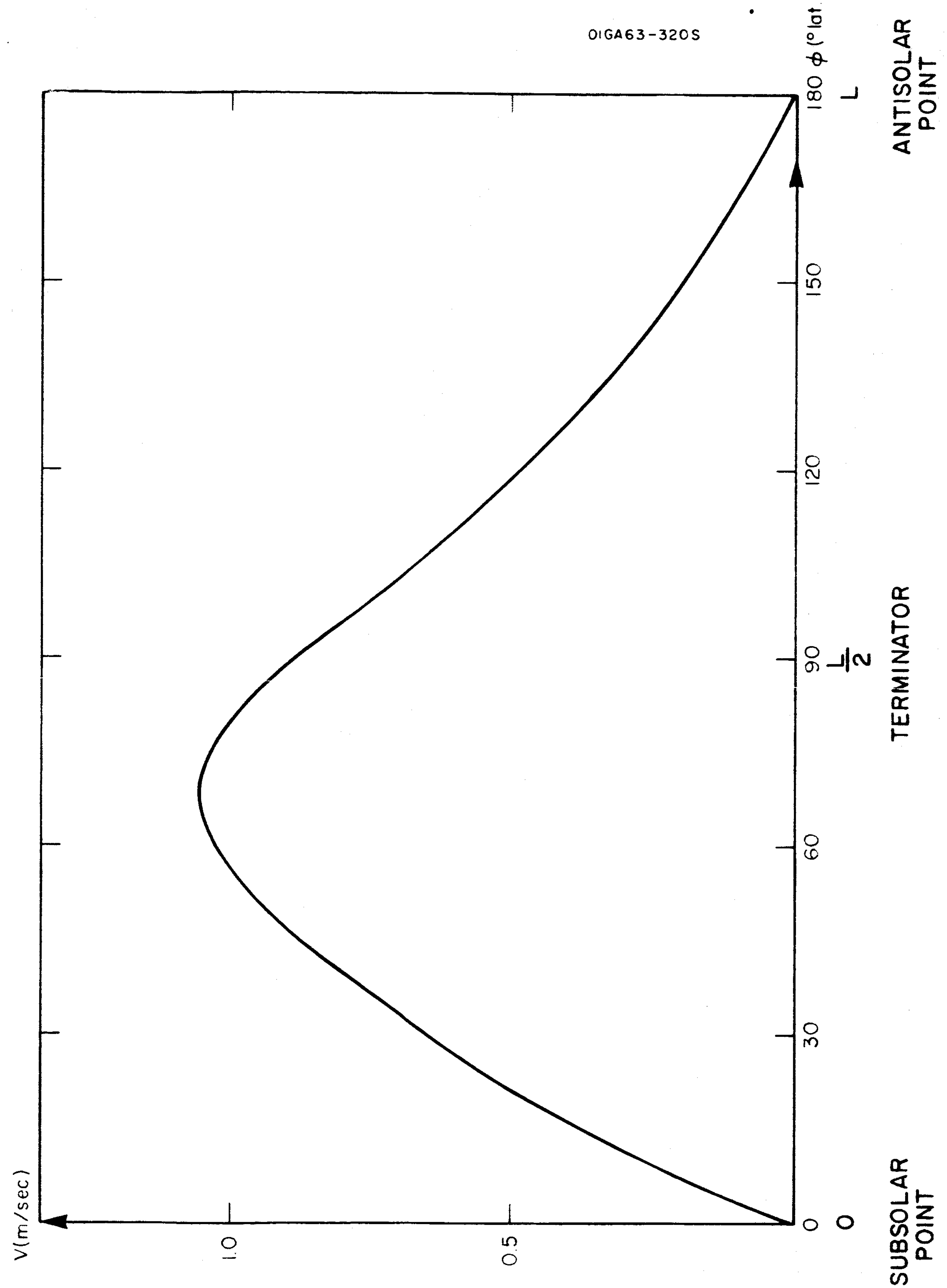

Figure 2. Horizontal distribution of velocity v with latitude.

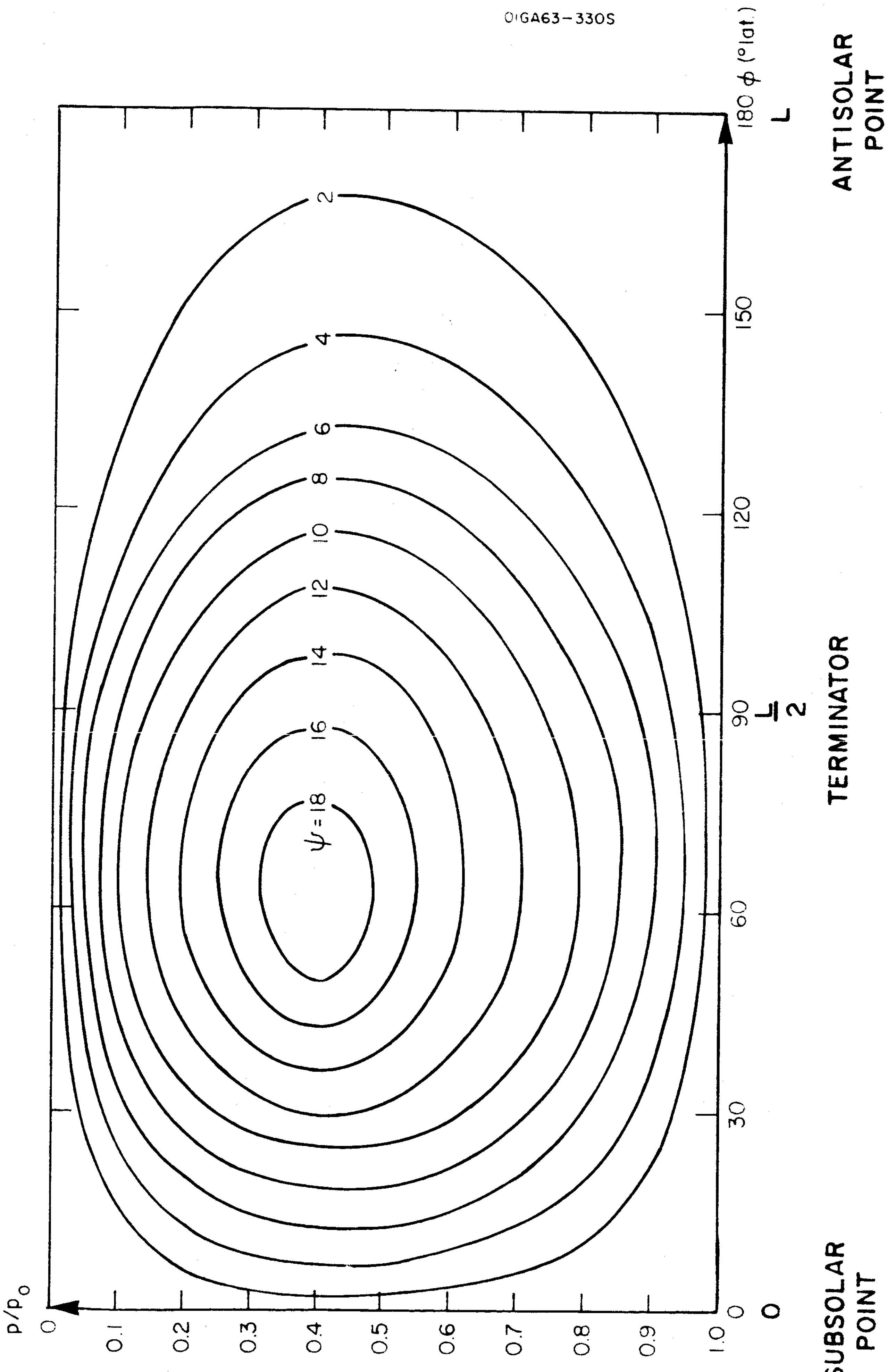

Figure 3. Stream field (ψ is in unit of 2.33×10^{-8} gm sec^{-3}).

terminator but on the sunlit side at somewhere between 60° and 70° latitude on our scale. The center of the vertical circulation is also located at the same latitude and the circulation is not symmetrical. The asymmetry of the circulation is probably due to the asymmetry of the gradient of the non-adiabatic heating. This asymmetry probably causes a strong upward flux of heat in the area immediately surrounding the sub-solar point. Since no net energy can be retained in a horizontal slice, the area of upward motion is smaller than the area of downward motion. As to the asymmetry in the vertical direction, it is mainly related to the vertical profile of the non-adiabatic heating function, Q, which we assumed to be asymmetrical for mathematical simplicity. Further investigation of the radiational heating function in the Venusian atmosphere is necessary. If the maximum intensity of the heating function is shifted downward in the atmosphere, then the entire circulation pattern would also shift downwards.

The range of wind velocity estimates shown in Table 1 serves to indicate the present uncertainty in wind velocities in the Venus atmosphere. It is hoped that this range can be narrowed down by refinement of the models.

SECTION 3

METEOROLOGY OF MARS

3.1 ESTIMATION OF MAXIMUM WIND NEAR THE SURFACE

A landing vehicle descending through the Martian atmosphere will be subject to horizontal transport by the prevailing atmospheric winds. If there are surface relief features on the planet, such a horizontal transport may lead to possible damage of the vehicle as it is carried horizontally to a collision with the solid surface. To properly design for such a possibility, it is desirable to have an estimate of the maximum wind likely to be encountered near the surface. We have started to look into the problem of estimating maximum winds near the surface.

The strongest surface wind velocities in the terrestrial atmosphere are found in tornadoes and typhoons or hurricanes. An expression for estimating the maximum surface wind speed for a convective vortex, such as a hurricane, has been derived by Kuo (1959).

$$v_{max} = \left\{ \frac{2\gamma R T_o}{\gamma - 1} \left[1 - \left(\frac{p_o}{p} \right)^{\kappa} \right] \right\}^{\frac{1}{2}}$$

where v_{max} = maximum tangential velocity.

$\gamma = \frac{c_p}{c_v}$ = the ratio of specific heat at constant pressure to the specific heat at constant volume.

R = gas constant for the atmosphere.

p_c = surface pressure at center of the vortex.

p_o = surface pressure at a distance where the wind velocity is zero.

κ = poisson constant = $\frac{c_p - c_v}{c_p}$.

T_o = surface temperature.

In a hurricane, the lowest surface center pressure is probably about 950 mb and the surface pressure p_o is 1000 mb. When the sea surface temperature, T_o, is 290°K, the maximum wind speed, from the above formula, is about 94 m/sec. This is comparable to the maximum observed wind speeds in hurricanes. On Mars, the noon-time temperature in the equatorial area is about 280°K. The center pressure of a vortex corresponding to a tropical storm on Mars has not been determined. However, a disturbance of surface pressure in a range of 2 to 3 mb in the equatorial area of Mars may be possible. If the center pressure is 2 mb lower than the surrounding surface pressure (p_o = 25 mb) and κ is the same as on Earth, the corresponding maximum surface wind velocity in the vortex is approximately

$$V_{max} = 114 \text{ m/sec.}$$

For p_c = 3 mb, V_{max} is approximately

$$V_{max} = 140 \text{ m/sec.}$$

Both wind speeds are larger than the wind speed in a hurricane on Earth. From the governing equation of maximum velocity, it is noticed that the dominating factor is the ratio of the center pressure to the surrounding pressure. Since the latest estimate of surface pressure on Mars is about 25 mb, a slight disturbance will create a severe wind storm. To obtain a maximum wind equal to the maximum wind speed computed for a hurricane on Earth, a central pressure of 23.75 mb is required. It remains to be answered whether a drop of 1.25 mb in the surface pressure of a Martian storm is likely. If large parts of the Martian surface are covered with sand, the heating and cooling by radiation will be rapid. Such conditions will lead to strong vertical convection. Yellow clouds are frequently observed at heights greater than 10 km. This implies storms of great vertical development and horizontal intensity. A drop of 1 to 3 mb in the center, compared to the mean surface pressure of 25 mb, is a likely possibility under such conditions.

Now let us seek a second method of estimating the maximum surface wind on Mars. An analysis of the observations of the places of origination and the movements of yellow cloud systems on Mars suggests that their behavior is quite similar to hurricanes on the Earth. The size of a yellow cloud system on the first observation of a series (DeVaucouleurs, 1954) on the date October 11, 1911 is about 500 km in radius. Then the radius of the tropical storm on Mars (here we define the radius of a storm as the distance from the center to a point on the circumference at which the tangential wind velocity is nearly zero) is probably very close to this value. If we use this value for the radius of the assumed tropical storm, and assume that the center pressure of this storm is 3 mb lower than the average surface pressure, and that the surface density is 5×10^{-5} g/cc, then, from the gradient wind formula for a cyclonic vortex at about 15° latitude ($f = 0.38 \times 10^{-4}$/sec), the cyclonic wind velocity in the tropical storm can be calculated. The mean wind velocity is

$$\bar{v} = \frac{\bar{r}f}{2}\left[\left(1 + \frac{4}{\bar{r}f^2}\,\frac{1}{\rho}\,\frac{\partial p}{\partial r}\right)^{\frac{1}{2}} - 1\right]$$

where $\bar{v}$ = mean wind velocity, corresponding to the wind at $r = \bar{r} = \frac{r_o}{2}$.

r = distance from center.

$\bar{r}$ = mean radius = $\frac{r_o}{2}$.

r_o = radius of the system.

f = Coriolis parameter.

ρ = density.

p = pressure.

Based on the values of the parameters presented above, the mean velocity in the storm is about

$$\bar{v} \approx \left[\bar{r} \frac{1}{\rho} \frac{\partial p}{\partial r} \right]^{\frac{1}{2}} = 52 \text{ m/sec} .$$

If we assume that the wind velocity increases linearly with distance from a value of zero at the edge of the storm to its maximum value at the center of the storm, we can obtain an estimate of the maximum wind by simply doubling the value of the computed average wind. This results in a value of 104 m/sec for the maximum wind, which is in general agreement with the value of 140 m/sec obtained, for a similar pressure drop, with the maximum wind formula discussed previously.

Since the estimates of the maximum wind speed based on the pure theoretical approach and on the size of an observed dust storm are in reasonable agreement, the estimate of a maximum surface wind speed of about 140 m/sec and a center pressure of the storm of about 22 mb, which is 3 mb less than the mean surface pressure, 25 mb, is plausible.

Although the above discussion indicates how an estimate of the maximum surface wind on Mars can be derived, there is no indication of what percentage of the time such winds may occur. For design purposes, it is usually desirable to have an estimate of the frequency of occurrence of high winds. The following discussion indicates how such estimates may be obtained.

Recently, Ryan (1964) and Gifford (1964) have presented estimates of the minimum wind speeds necessary to initiate dust storms in the Martian atmosphere. The yellow clouds in the Martian atmosphere are generally believed to be manifestations of such dust storms. The minimum velocities obtained by these authors for a height of one meter above the surface are listed in Table 2.

TABLE 2

Minimum horizontal wind speed at a height of 1 meter necessary to initiate dust storm (km hr^{-1}).

Ryan (1964)					Gifford (1964)		
	Surface Model 1		Surface Model 2				
k(cm)	80 mb	25 mb	80 mb	25 mb	k(cm)	100 mb	10 mb
0.03	40	95	60	145	0.3	14	72
0.006	--	--	70	180	---	--	--
0.003	--	--	75	190	---	--	--

In Table 2, k is a measure of the surface roughness, the pressures refer to the surface pressure on Mars, and Ryan's Models 1 and 2 refer to different assumptions about the Martian surface. The variation in speeds between Ryan's surface model 1 and Gifford's model is mainly due to the difference in assumed surface roughness, although differences in surface pressure and other necessary constants also contribute to the variation between the two authors. Regardless of the variation in wind speed among the different models, the important thing is that these authors have developed a model for estimating the threshold wind speeds near the surface that are required to initiate dust storms. If we assume that whenever such a wind speed occurs on Mars, a dust storm and yellow cloud will result, then, by determining the frequency of occurrence of yellow clouds, we can estimate the frequency of occurrence of the threshold wind speeds.

Yellow clouds are known to be a rare occurrence on Mars. However, until recently no one has ever given a quantitative estimate of frequency of occurrence. Recently, Gifford (1964) estimated that yellow clouds displaying motion occur slightly more than once per opposition period. This estimate was based upon a search of the literature, and files and publications of various observatories. Over a period of 87 years, only 53 examples of yellow cloud motion could be found. Let us assume that a reasonable estimate of the occurrence of yellow clouds is once per opposition period. To be conservative, let us further assume that observations of Mars are only made during a two-month period around opposition, and that all the reported observations of yellow clouds occurred during these two-month periods. This assumption leads to an estimate of one yellow cloud every sixty days. If we assume that the average yellow cloud lasts one day and that the wind speeds necessary to initiate the cloud last just as long, we can estimate that threshold wind speeds occur 1/60 of the time. This means that 59/60 ths of the time the wind speeds are less than the threshold value. This type of argument can be refined further by taking into consideration the area covered by the average yellow cloud and favored locations of occurrence on the planet. However, before making such refined estimates, we should attempt to resolve some of the differences in estimated threshold wind speeds. An attack on this problem is planned for the next quarter.

SECTION 4

METEOROLOGY OF JUPITER

4.1 VERTICAL VARIATION OF RADIATIVE EQUILIBRIUM TEMPERATURES ABOVE CLOUDS

The presence and approximate amounts of ammonia and methane above the clouds of Jupiter have been deduced from spectroscopic observations. Both of these gases have absorption bands in the infrared region of the spectrum and should play an important role in shaping the vertical distribution of radiative equilibrium temperature above the cloud-top. The absorption coefficients of these gases are wavelength dependent. Therefore, to compute the radiative equilibrium temperature distribution, we would like to develop a non-grey radiative transfer model applicable to the Jupiter atmosphere.

We can divide the infrared region into a finite number of spectral intervals, in each of which the absorption coefficient can be considered constant. For each spectral interval, we will have a different opacity, as follows:

$$\begin{aligned} \tau\ (z) &= k_1 \int_0^z \rho dz \\ \tau_2(z) &= k_2 \int_0^z \rho dz \\ \tau_n(z) &= k_n \int_0^z \rho dz \end{aligned} \qquad (24)$$

where τ is opacity, z is height, k is the absorption coefficient, and ρ is density of absorbing gas. We can relate the opacities of all spectral intervals to a reference opacity, for example, to the opacity of the first spectral interval by the formula

$$\tau_n(z) = \frac{k_n}{k_1}\,\tau(z) = w_n\tau(z)$$

where w_n is the ratio of the absorption coefficient in the nth spectral interval to the absorption coefficient in the reference spectral interval. The flux of radiation at the opacity level τ at height z can then be written as

$$F(\tau) = F_1(\tau) + F_2(w_2\tau) + \ldots . F_n(w_n\tau). \qquad (25)$$

The condition for radiative equilibrium requires that

$$\frac{dF(\tau)}{d\tau} = 0 , \qquad (26)$$

which can be written as

$$\frac{d}{d\tau}\left[F_1(\tau) + F_2(w_2\tau) + \ldots . F_n(w_n\tau)\right] = 0. \qquad (27)$$

The expressions for the fluxes of radiation at the level τ for the various spectral regions can be written as

$$F_1(\tau) = 2B_1(o)E_3(\tau) + 2\int_o^{\tau} B_1(t)E_2(\tau - t)dt - 2\int_{\tau}^{\tau_g} B_1(t)E_2(t - \tau)dt$$

$$F_2(w_2\tau) = 2B_2(o)E_3(w_2\tau) + 2\int_o^{w_2\tau} B_2(t)E_2(w_2\tau - t)dt$$

$$- 2\int_{w_2\tau}^{w_2\tau_g} B_2(t)E_2(t - w_2\tau)dt \qquad (28)$$

$$F_n(w_n\tau) = 2B_n(o)E_3(w_n\tau) + 2\int_o^{w_n\tau} B_n(t)E_2(w_n\tau - t)dt$$

$$- 2\int_{w_n\tau}^{w_n\tau_g} B_n(t)E_2(t - w_n\tau)dt$$

where $B_1(o)$, $B_2(o)$, and $B_n(o)$ are the black-body fluxes radiated by the cloud-top in the 1st, 2nd, and nth spectral region; the E's are exponential integrals, and τ_g is the opacity of the entire atmosphere above the cloud-top in the reference spectral interval. After applying the radiative equilibrium condition (27) and simplifying, one can obtain the following expression

$$B_1(\tau) + w_2B_2(w_2\tau) + \dots w_nB_n(w_n\tau) =$$

$$+ \tfrac{1}{2}\left[B_1(o)E_2(\tau)+B_2(o)w_2E_2(w_2\tau)+ \dots B_nw_nE_2(w_n\tau)\right]$$

$$+ \tfrac{1}{2}\int_o^{\tau_g}\Big[B_1(t)E_1(|\tau-t|) + B_2(t)w_2{}^2E_1(w_2|\tau-t|)$$

$$+ \dots B_n(t)w_n{}^2E_1(w_n|\tau-t|)\Big] dt \quad . \qquad (29)$$

At a particular level, τ, in the atmosphere, the black-body fluxes in each spectral interval depend solely on the temperature at that level and can be determined from Planck's law. Thus, if one divides the atmosphere into m levels, one can write an equation similar to (29) for each level. There would be (m+1) unknowns — the temperature at the cloud-top and the temperatures at each of the m levels above the cloud-top. By imposing the condition that the outgoing infrared radiation must balance the incoming solar radiation at the top of the atmosphere, we can obtain an additional equation that makes it possible to solve for the unknown cloud-top temperature and the m unknown atmospheric temperatures. The equation of balance at the top of the atmosphere can be written as

$$2\left[B_1(o)\ E_3(\tau_g) + B_2(o)\ E_3(w_2\tau_g) + \ldots B_n(o)\ E_3(w_n\tau_g)\right]$$

$$+ 2\int_o^{\tau_g} \left[B_1(t)E_2(\tau_g - t) + B_2(t)E_2(w_2|\tau_g - t|) + \ldots B_n(t)E_2(w_n|\tau_g - t|)\right]dt$$

$$= \sigma\, T_e^{\,4} \qquad (30)$$

where T_e is the effective temperature of the incoming solar radiation and σ is the Stefan-Boltzmann constant. Given T_e and the variation of absorption coefficient with wavelength, it is possible to determine, from the numerical analogues of (29) and (30), the radiative equilibrium temperature distribution from the cloud-top to the top of Jupiter's atmosphere. Computer programming of this model will begin in the next quarter.

REFERENCES

DeVaucouleurs, G., 1954: Physics of the Planet Mars. Faber and Faber Limited, London, 365pp.

Geophysics Corporation of America, 1964: Planetary meteorology, Quarterly Progress Report No. 1, Contract No. NASw-975.

Gifford, F. A., Jr., 1964: A study of Martian yellow clouds that display movement, Monthly Weather Review, Vol. 92, 10, 435-440.

Kuo, H-L., 1959: Dynamics of convective vortices and eye formation. The atmosphere and the sea in motion. The Rockefeller Institute Press in association with Oxford University Press, New York, 509pp.

Mintz, Y., 1962: The energy budget and atmospheric circulation on a synchronously rotating planet. Memorandum RM-3243-JPL, The Rand Corporation, Santa Monica, California.

Ryan, J. A., 1964: Notes on the Martian yellow clouds. J. Geophysical Res., Vol.69, 18, 3759-3770.